JOURNAL OF VIROLOGY, July 1992, p. 4242–4251
0022-538X/92/074242-10$02.00/0

Vol. 66, No. 7

Two Distant Upstream Regions Containing *cis*-Acting Signals Regulating Splicing Facilitate 3′-End Processing of Avian Sarcoma Virus RNA

JENNIFER T. MILLER AND C. MARTIN STOLTZFUS*

Department of Microbiology, University of Iowa, Iowa City, Iowa 52242

Received 12 December 1991/Accepted 2 April 1992

Retroviruses, pararetroviruses, and related retrotransposons generate terminally redundant RNAs by transcription of a template flanked by long terminal repeats in which initiation occurs within the 5′ long terminal repeat sequences and 3′-end processing occurs within the 3′ long terminal repeat sequences. Processing of avian sarcoma virus RNA is relatively inefficient; approximately 15% of the viral RNA transcripts are read-through products; i.e., they are not processed at the viral poly(A) addition site but at sites in the cellular sequence further downstream. In this report, we show that the efficiency of processing at the viral site is further reduced by deletion of two distant upstream sequences: (i) a 606-nucleotide sequence in the *gag* gene containing a *cis*-acting negative regulator of splicing and (ii) a 136-nucleotide sequence spanning the *env* 3′ splice site. The deletion of either or both upstream regions increases the levels of read-through products of both unspliced and spliced viral RNA. In contrast, deletion of the *src* 3′ splice site does not affect the efficiency of processing at the viral poly(A) addition site. The effects on 3′-end processing are not correlated either with distance from the promoter to the poly(A) addition site or with the overall level of viral RNA splicing. Substitution of the avian sarcoma virus poly(A) signal with the simian virus 40 early or late poly(A) signal relieves the requirement for the distant upstream sequences. We propose that cellular factors, which may correspond to splicing factors, bound to the upstream viral sequences may interact with factors bound at the avian sarcoma virus poly(A) signal to stabilize the polyadenylation-cleavage complex and allow for more efficient 3′-end processing.

Primary RNA transcripts of viral and cellular eukaryotic genes are subject to a number of posttranscriptional processing steps, including capping, methylation, splicing, 3′ cleavage, and polyadenylation. The processing at the 3′ terminus occurs by endonucleolytic cleavage followed by the addition of approximately 200 adenylic acid residues (63). Several *cis*-acting elements have been shown by mutational analysis in vivo to be essential for these steps to occur. These elements include the hexanucleotide AAUAAA located 10 to 20 nucleotides (nt) 5′ of the poly(A) addition site (17, 35, 40, 62) and a less conserved GU- or U-rich element 3′ of the poly(A) addition site (5, 14, 18, 33, 44, 49, 64). In several specialized cases, signals upstream of the hexanucleotide element that may be important in regulation of polyadenylation-cleavage efficiency have been reported (9, 10, 12, 15, 16, 42, 43, 46, 57). In addition, in transcription units in which multiple polyadenylation signals are present, alternative splicing may promote the use of one poly(A) site, with the exclusion of the other (1, 8, 20, 31, 38, 64).

Many retroviruses, pararetroviruses, and retrotransposons also demonstrate a type of regulated polyadenylation. Proviral DNA genomes are flanked by long terminal repeats (LTRs), each of which contains the signals for initiation of transcription and 3′-end processing. In most retroviruses, transcription results in a terminally redundant RNA that contains two poly(A) signals. One of these signals arises from sequences in the 5′ LTR, and the other signal arises from identical sequences in the 3′ LTR. However, only the downstream signal is used as a processing site. Pararetroviruses and retrotransposons synthesize primary transcripts with a similar arrangement of two poly(A) signals (6, 39). Several mechanisms have been proposed to account for the selective use of the downstream signal. These mechanisms have been shown to include, first, the presence of additional signals upstream of the hexanucleotide element in the unique viral sequences which are necessary for 3′-end processing (9, 16, 42, 43, 46, 57) and, second, promoter occlusion in which the efficiency of 3′-end formation is determined by the distance from the promoter to the poly(A) addition site (25, 47, 60).

Avian sarcoma and leukosis viruses (ASV and ALV, respectively) have evolved an LTR arrangement that avoids this general problem by positioning the 5′ start site for transcription between the upstream AAUAAA and the downstream GU-rich element. Therefore, in the terminally redundant primary transcript, there is only one functional poly(A) signal, which arises from sequences in the 3′ LTR. However, in infected cells, a high level of viral transcripts that are processed in cellular sequences downstream of the viral 3′ LTR poly(A) site are present (21). This somewhat-less-efficient level of 3′-end processing relative to other viral polyadenylation-cleavage efficiencies (7, 10, 32) has implications for the biology of ALV. Some cellular oncogenes (e.g., *myb* and *erbB*) are activated by adjacent upstream ALV proviral integration followed by read-through transcription into the cellular sequences (26, 41). One model suggests that some cellular oncogenes may have been transduced by packaging such hybrid read-through transcripts into ALV virions followed by recombination with wild-type viral RNAs during a subsequent round of reverse transcription (22, 56).

In an effort to understand the basis for the relatively inefficient ASV and ALV 3′-end processing, we have devel-

* Corresponding author.

oped a transfection assay that measures the level of read-through transcription in cells transfected with wild-type and mutant proviral DNA. We have found two regions in the unique viral sequences and distant from the viral poly(A) addition site that positively affect 3'-end processing. Both of these regions contain *cis* signals affecting viral RNA splicing. Our results suggest, however, that the efficiency of 3'-end processing at the viral poly(A) site is not coupled to the act of splicing itself. We propose that the presence of the upstream *cis* signals affecting splicing in the full-length transcript may facilitate 3'-end processing at the viral poly(A) site.

MATERIALS AND METHODS

Plasmids. The clones used in this study are diagrammed in Fig. 2. pJD100, an infectious nonpermuted clone of a Prague A strain of ASV cloned at the *Hin*dIII site of pBR322, was obtained as a gift from J. Thomas Parsons, Department of Microbiology, University of Virginia, Charlottesville. pUC18.Bgl.SVA contains a trimer of a 237-nt fragment containing the simian virus 40 (SV40) early and late gene poly(A) signals contained in pUC18 and was obtained as a gift from Ian Maxwell, University of Colorado Health Science Center, Denver. Plasmids pΔ11 3'CAT, pΔ9, pΔ5-14 3'CAT, pJS2CAT (52), pΔ5-25 3'CAT, p5'XH1 (54), and pMPM7 and pMPM13 (4) have been described previously. The clone pSLB-Sac(−23) (4), previously reported to contain a deletion of 23 bases from nt 6870 to 6892 was reanalyzed and found to contain a deletion of 22 bases from nt 6871 to 6892. Deletion and inversion mutants were created by standard recombinant DNA techniques (45). pJTM14 was created by cloning the entire provirus derived from pJD100 into a pUC18-based vector (pSVEUCAT) containing the *cat* gene and the SV40 early poly(A) signal. pSVEUCAT was obtained from L. Turek, Department of Pathology, University of Iowa. pJTM19 was constructed by ligation of a *Bgl*II fragment (nt 4236 to 7736) into pΔ11 3'CAT. pJTM28 and pJTM29 were constructed by partial digestion of pJTM14 with *Nhe*I and complete digestion with *Kpn*I. The ends were blunt ended with T4 DNA polymerase and ligated. pJTM21 was created by digestion of pJTM14 with *Sac*II. pJTM50 was constructed by ligation of the *Sac*II fragment (nt 543 to 1806) back into the wild-type pJTM14 in the reverse orientation. pJTM54 was created by ligation of a *Sac*II fragment (nt 543 to 1806) from pΔ9 into pJTM21. pJTM46 was constructed by ligation of a *Kpn*I-*Mlu*I fragment (nt 4995 to 7901) from pSLB-Sac(−23) into the wild-type pJTM14. pJTM6 was created by ligation of a *Cla*I linker into pΔ11 3'CAT partially digested to a linear fragment with *Eco*RI at nt 9238. pJTM52 was constructed by ligation of a *Sac*I-*Hin*dIII fragment (nt 6865 to 9393) from pJTM6 into pSPT18. pJTM53 was constructed by ligation of a *Hin*dIII-*Sma*I fragment (289 nt) from pUC18.Bgl.SVA into pJTM52 cleaved with *Hin*dIII and *Cla*I. This linear fragment was blunt ended with T4 DNA polymerase and ligated. pJTM56 was constructed by partial digestion of pJTM53 with *Bgl*II and complete digestion with *Bam*HI, followed by religation of both fragments created by the digestion. pJTM58 was created by ligation of an *Mlu*I-*Hin*dIII fragment from pJTM56 into pΔ5-25 3'CAT. pJTM60 was constructed by ligation of an *Mlu*I-*Sac*I fragment from pJTM14 into pJTM58. pJTM62 was created by cleavage of pJTM60 with *Sac*II followed by religation of both fragments, created by the digestion, and by selection for insertion of the inverted fragment.

Cell culture and DNA transfections. Secondary chicken embryo fibroblasts (CEF) isolated from embryonated eggs that were negative for both group-specific antigen and chicken-helper factor (SPAFAS, Inc., Norwich, Conn.) were cultured in SGM (Medium 199 [Bethesda Research Laboratories, Inc., Gaithersburg, Md.] supplemented with 10% (vol/vol) tryptose phosphate broth and 5% (vol/vol) calf serum]. CEF were transfected by using a DEAE-dextran procedure described previously (50). Purified plasmid DNA (40 μg) in 13 ml of serum-free SGM adjusted to a final concentration of 50 mM Tris (pH 7.4) was used to transfect CEF on subconfluent 150-mm plates at a concentration of 200 μg of DEAE-dextran per ml. After 25 min at room temperature, 4 ml of the transfection mix was removed, and 21 ml of serum-free SGM was added. The plates were incubated for 3 h at 37°C and then refed with 25 ml of SGM. The medium was replaced 20 to 24 h later with 25 ml of fresh SGM. RNA stability was determined by the addition of 10 ml of SGM containing 1 μg of dactinomycin per ml to confluent CEF on 100-mm plates 48 h after transfection. Whole-cell RNA was harvested (see below) at 0, 3, 6, 9, and 12 h after addition of the drug and analyzed by the RNase protection assay.

RNA isolation and analysis. Whole-cell RNA at 48 h after transfection was isolated by the guanidine hydrochloride method essentially as described by Strohman et al. (55). The poly(A)$^+$ RNA fraction was isolated by binding 50 to 100 μg of whole-cell RNA to an oligo(dT)-cellulose column (approximately 0.1 g) in the presence of 0.5 M NaCl and 0.05% sodium dodecyl sulfate (SDS). After a high salt (0.5 M NaCl) wash, the bound poly(A)$^+$ fraction was eluted in the presence of 0.05% SDS. This fraction was then reapplied to the column in the presence of high salt, washed, and reeluted as described above. Northern blot analysis of 10 to 20 μg of whole-cell RNA was performed according to the method of Sambrook et al. (45) and probed with an SP6 riboprobe (34). The RNase protection assay was carried out essentially as described previously (54), except that the hybridizations were performed at 57°C for 14 h under conditions of greater than 10-fold molar excess of riboprobe, determined empirically by hybridization of 10 μg of whole-cell RNA with increasing amounts of probe. The RNase digestions were done at 30°C for 1 h with 25 μg of RNase A per ml and 6,000 U of RNase T_1 per ml. The protected fragments were denatured by being heated at 85°C for 10 min and separated on a denaturing 7 M urea–5% polyacrylamide gel at 500 V for 4 to 5 h. Densitometric analysis was performed as described previously (4). Statistical analyses were obtained by using STAT PAC, Apple IIe software.

Materials. [α-^{32}P]UTP (800 Ci/mmol) was purchased from Amersham Corp., Arlington Heights, Ill. Restriction enzymes, T4 DNA polymerase, T4 DNA ligase, proteinase K, and plasmid pSPT18 were purchased from Boehringer Mannheim Biochemicals, Indianapolis, Ind. RNase T_1 and the 1-kb ladder were obtained from Bethesda Research Laboratories. Dactinomycin and RNase A were obtained from Sigma, St. Louis, Mo. SP6 polymerase was obtained from Promega Biotec Co., Madison, Wis. Oligo(dT)-cellulose was purchased from Collaborative Research, Inc., Waltham, Mass. The *Cla*I linker was obtained from New England Biolabs, Beverly, Mass.

RESULTS

Analysis of ASV 3'-end processing in transfected CEF. To define which elements affected 3'-end processing in ASV, we used a transient transfection assay to compare the level of

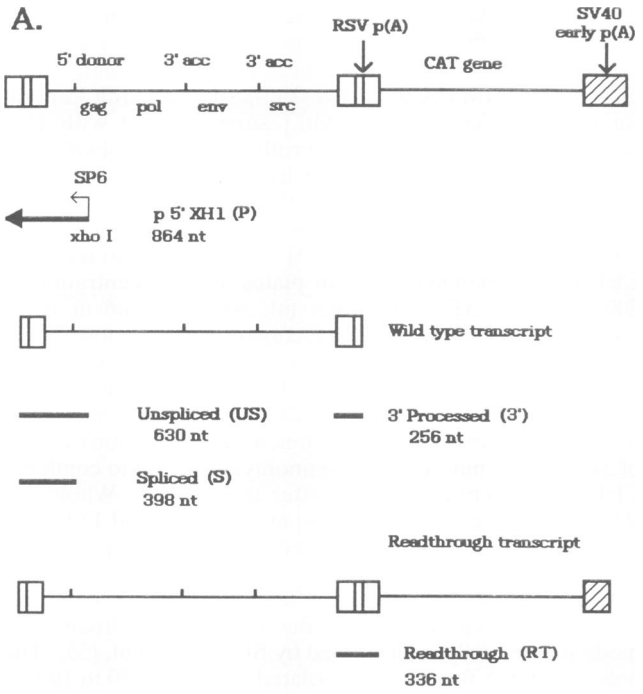

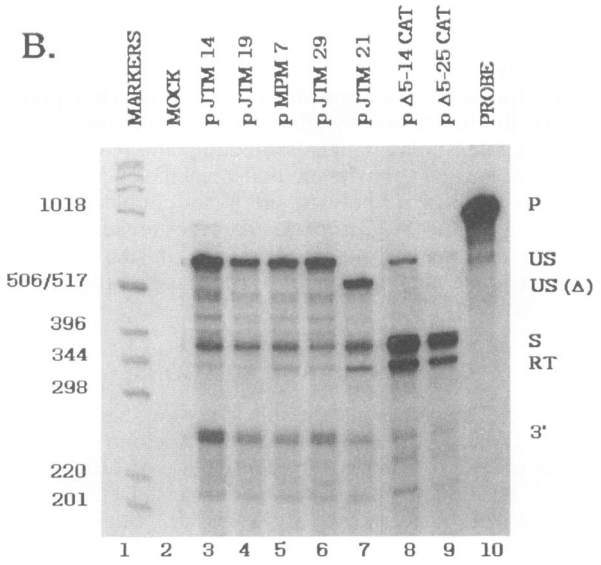

FIG. 1. RNase protection assays of wild-type and mutant RNA samples. (A) Map of riboprobe template and resulting protected fragments. The sizes of the expected fragments are indicated below the RNA species. Nucleotides were numbered according to the ASV Prague C sequence (48). (B and C) RNase protection assays showing the expected protected RNAs. Markers correspond to γ-^{32}P end-labelled DNA fragments of the 1-kb ladder (Bethesda Research Laboratories). The probe (P), unspliced (US), and spliced (S) hybrids are indicated, as well as the truncated unspliced band that results when constructs with deletions or inversions originating at nt 543 (*Sac*II) are assayed (US Δ). The bands corresponding to read-through RNA species (RT) and those processed at the viral 3′ LTR poly(A) site (3′) are also indicated.

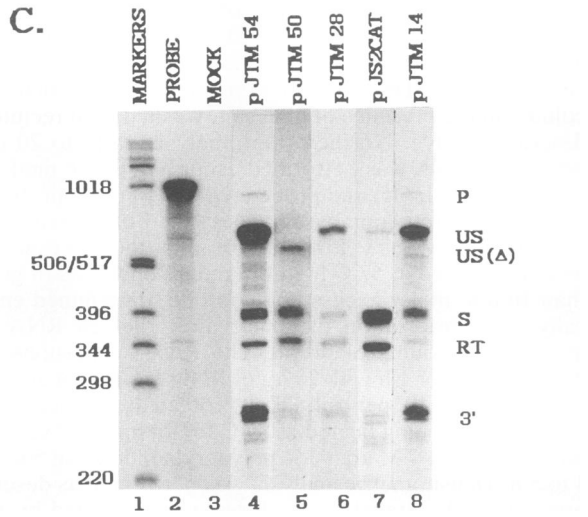

transcripts processed at the polyadenylation [poly(A)] site in the 3′ LTR with those resulting from read-through transcription. To provide a defined 3′ processing site and to confer stability to the transcripts not processed at the correct site, all constructs contained the bacterial chloramphenicol acetyltransferase (*cat*) gene followed by the SV40 early poly(A) signal cloned downstream of the provirus (Fig. 1A). CEF were transfected with genomic clones of ASV containing the above sequences. Forty-eight hours after transfection, whole-cell RNA was harvested and assayed by an RNase protection assay with an antisense riboprobe transcribed from the linearized DNA template p5′HX1 (Fig. 1A) under conditions of probe excess (see Materials and Methods). This probe protects LTR sequences present at the 3′ ends of the messages, producing fragments corresponding to transcripts that are processed at the ASV poly(A) site (256 nt), and read-through transcripts (336 nt). The probe is also complementary to sequences spanning the 5′ LTR, the splice donor site, and a portion of the *gag* gene extending to the *Xho*I site at nt 630. Therefore, the amounts of both unspliced (630 nt) and spliced (398 nt) transcripts can also be determined by the assay.

The amount of read-through RNA measured after transfection with the wild-type genomic clone, pJTM14, was similar to the results obtained by Herman and Coffin (21) for ALV-infected turkey embryo fibroblasts; approximately 15% of the viral RNA transcripts were not processed at the 3′ LTR poly(A) site (Fig. 1B, lane 3; Fig. 2). The level of viral read-through transcripts in the poly(A)$^+$ RNA was identical to that obtained for the whole-cell RNA (data not shown). Thus, the efficiency of 3′-end processing by the transient transfection assay correlated well with the efficiency of 3′-end formation in transcripts arising from integrated proviruses. This result also indicated that the downstream *cat* and SV40 sequences did not influence the efficiency of 3′-end processing in ASV.

Two distant upstream regions facilitate the efficiency of ASV 3′-end processing. Previous studies of regulation of RNA splicing in ASV indicated that two clones, pΔ5-14 3′CAT and pΔ5-25 3′CAT, deleted in a portion of *gag* and in all of *pol*, demonstrated increased levels of read-through transcription as well as increased levels of splicing (54). In addition, pΔ5-25 3′CAT was deficient in a substantial portion of *env*. Read-through transcription in these clones was elevated approximately 3- to 5-fold compared with that of the wild type (Fig. 1B, lanes 8 and 9, and summarized in Fig. 2). These data suggested that there might be distant upstream

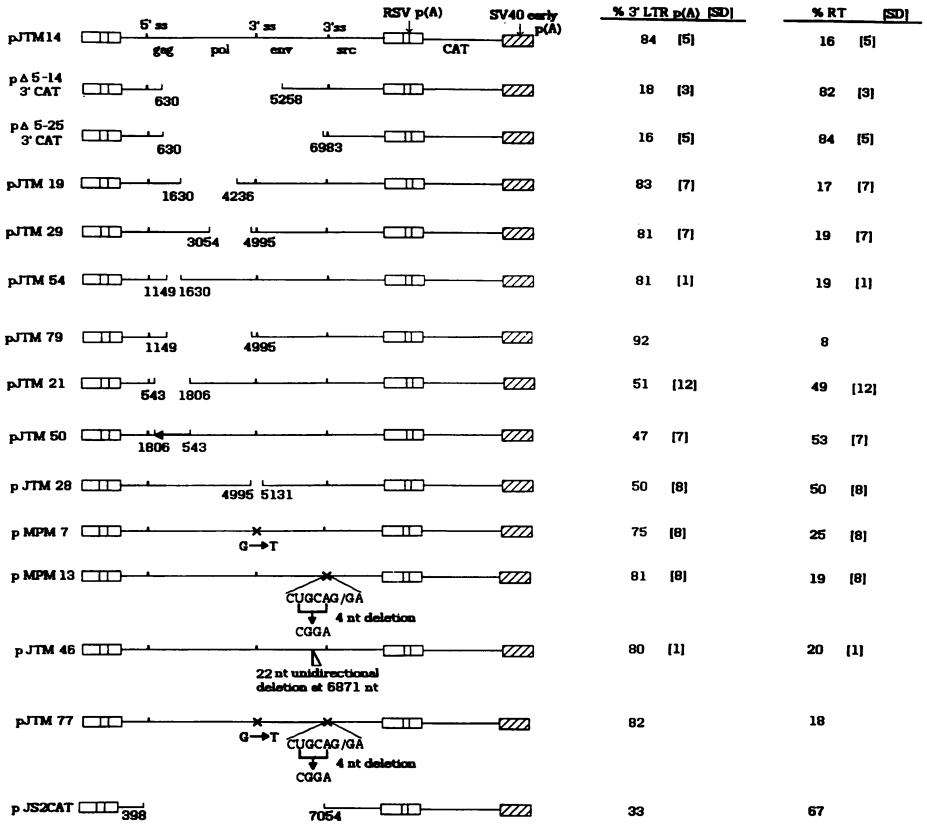

FIG. 2. Schematic representation of wild-type and mutant constructs and their corresponding levels of read-through RNA. Deletions are indicated by gaps in the solid line, with start and end points marked by the numbers of the respective nucleotides (numbered as described in the legend to Fig. 1). Thick arrow, inverted *Sac*II fragment in pJTM50; hatched box, SV40 early gene poly(A) signal. Note that pJS2CAT is a cDNA clone possessing an exact deletion of the *src* intron. Percentages of read-through (RT) and correctly processed RNA [3'LTR p(A)] were determined by densitometric analysis of bands resulting from the RNase protection assay (see Fig. 1B and C) and were adjusted to account for the molar ratio of uridine residues present as described previously (4). The standard deviation (SD) for each sample pair is indicated in brackets.

cis-acting sequences in the viral genome which influenced the site of 3'-end formation of ASV RNA.

In order to define more precisely the region(s) responsible for wild-type levels of 3'-end formation, mutants with smaller deletions in *gag* and/or *pol* were analyzed by the RNase protection assay. Mutants pJTM19 (Δ = nt 1630 to 4236), pJTM29 (Δ = nt 3054 to 4995) and pJTM54 (Δ = nt 1149 to 1630) exhibited no significant differences ($P > 0.4$) in the amounts of read-through transcription compared with that of the wild type (Fig. 1B, lanes 4 and 6; Fig. 1C, lane 4; Fig. 2). Taken together, these data indicate that sequences contained within nt 1149 to 4995 do not contain *cis*-acting sequences that affect wild-type levels of 3' processing. To confirm this conclusion, a mutant (pJTM79) in which the entire region from nt 1149 to 4995 was deleted produced levels of read-through RNA that were not elevated and were comparable to those of the wild type (Fig. 2).

Mutations in two regions of the viral genome were associated with significantly increased levels of read-through RNA. Either deletion (pJTM21) or inversion (pJTM50) of a 1263-nt *Sac*II fragment from nt 543 to 1806 resulted in levels of read-through RNA which were threefold higher than that of the wild type (Fig. 1B, lane 7; Fig. 1C, lane 5; Fig. 2). As previously shown (2, 54), these mutations also resulted in an increased level of viral RNA splicing. The ratio of spliced RNA to unspliced RNA with the inversion mutant is larger than the ratio obtained with the deletion mutant (compare Fig. 1B, lane 7, and C, lane 5). This result was expected because the inversion creates a premature stop codon in the *gag* gene, which has been shown to selectively destabilize the unspliced RNA (2). These results, together with the data given above, suggest the presence of an orientation-dependent element affecting 3' processing contained in the sequences from nt 630 to 1149 (region I). The distance from the promoter in the 5' LTR to the viral poly(A) site in the inversion mutant was unchanged; this finding suggested that the elevated levels of read-through RNA obtained with the deleted constructs were not due to the reduced distance from the cap site to the poly(A) site in the 3' LTR.

The region downstream of nt 4995 was also studied. The genomic clone pJTM28 contained a 136-nt deletion from nt 4995 to 5131 and demonstrated increased levels of read-through RNA similar to those of the region I mutants (Fig. 1C, lane 6; Fig. 2). As shown previously, this mutation resulted in wild-type levels of splicing; however, all of the splicing occurred at the *src* 3' splice site (3' ss) (4). Again, the fact that the distance from the cap site to the poly(A) site in pJTM28 was greater than that of several other constructs (pJTM54, pJTM19, and pJTM29) demonstrating wild-type levels of read-through products indicated that a reduction in this distance was not correlated with increased levels of read-through RNA.

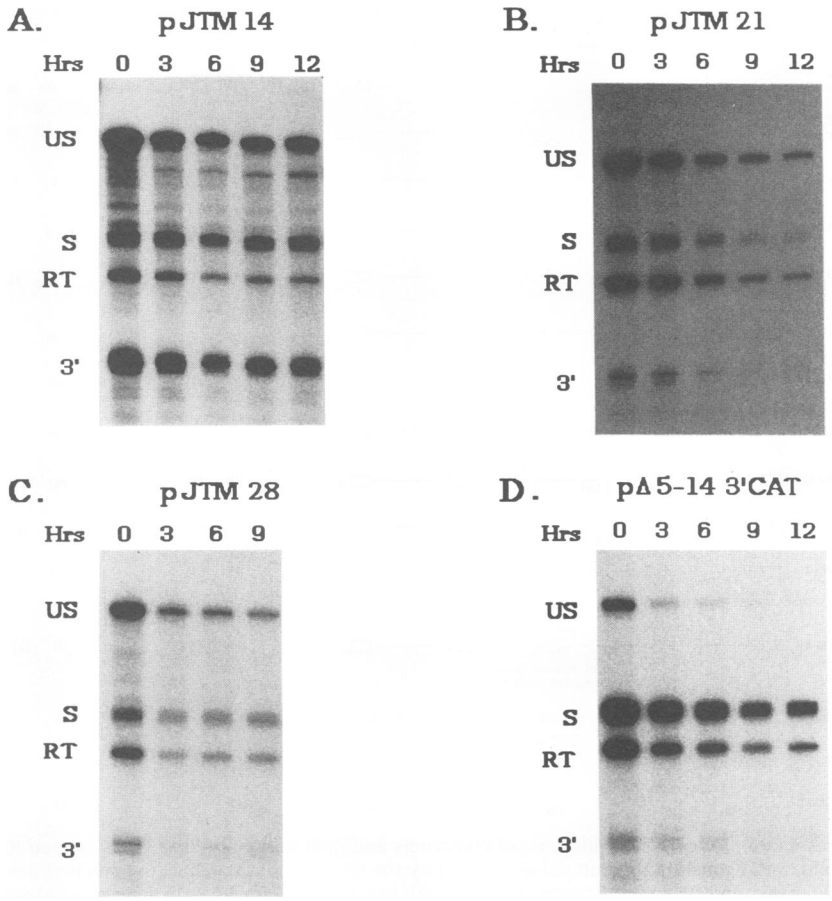

FIG. 3. Analysis of RNA stability in CEF transfected with wild-type and mutant constructs. Steady-state levels of the wild type (A), a region I deletion (B), a region II deletion (C), and a region I plus region II deletion mutant (D) are shown. RNA at various times after the addition of dactinomycin (1 μg/ml) as determined by the RNase protection assay is shown. The identities and locations of the protected RNAs are as indicated in the legend to Fig. 1.

It was also possible, however, that the deleted sequences in region I or II functioned to stabilize the correctly processed messages. In order to examine this possibility, time course studies utilizing dactinomycin, an inhibitor of RNA synthesis, were performed with the wild-type clone, a region I deletion mutant (pJTM21), a region II deletion mutant (pJTM28), or a construct which removed both regions (pΔ5-14 3′CAT). The drug was added 48 h after transfection; whole-cell RNA was harvested at 0, 3, 6, 9, and 12 h postaddition; and the samples were assayed by RNase protection for levels of correctly processed and read-through transcripts (Fig. 3). The steady-state levels of RNAs processed at the 3′ LTR and the read-through RNAs at various times after addition of the drug are given in Table 1. The ratios of read-through to correctly processed RNAs in the deleted clones remained relatively constant at the various chase times, indicating that the mutations did not cause a selective degradation of transcripts processed at the ASV poly(A) site. In contrast, note in Table 1 that the ratios of spliced RNA to unspliced RNA for pJTM14, pJTM28, and pΔ5-14 3′CAT increased over time, as expected from the previous data indicating that the unspliced RNA is more labile than the spliced RNAs (2, 53). These data suggested that the read-through transcripts were present in both the spliced and unspliced pools of RNA. This fact was confirmed by Northern blot analyses (see below). Surprisingly, as shown in Table 1, the ratio of spliced RNA to unspliced RNA for pJTM21 did not increase significantly during the dactinomycin chase. We do not yet understand this difference compared with those of the other mutants, and it is currently under investigation in our laboratory.

Analysis of poly(A)$^+$ RNA isolated from CEF transfected with mutants containing deletions spanning region I or II (data not shown) gave results similar to those shown in Fig. 2, indicating that the read-through transcripts are polyadenylated at a downstream site and that these RNAs do not arise as a result of aberrant transcription termination.

3′-end processing efficiency is not directly coupled to the act of RNA splicing. Both regions that influenced 3′-end processing contained signals affecting splicing of the viral RNA. Region II contained the *env* 3′ ss at nt 5078 (11) and also part of an exon sequence necessary for maintenance of wild-type splicing levels (29); region I contained a *cis*-acting negative regulator of splicing (NRS) (2, 54). Thus, we tested whether the act of RNA splicing was directly coupled to 3′-end processing. First, we tested a mutant (pMPM7, Fig. 2) containing a G-to-T point mutation at the consensus AG of the *env* 3′ ss, which abolishes *env* splicing. In cells transfected with this mutant, the overall level of viral RNA splicing does not change; however, the proportion of RNA normally spliced at *env* is shifted to *src* (4). The levels of read-through transcription obtained with this clone were

TABLE 1. Comparison of levels of spliced and unspliced RNAs and 3' processed RNA at various times after dactinomycin treatment[a]

Plasmid	Time[b] (h)	% RNA processed		SD[c]	% RNA		SD
		At 3' LTR	As RT[d]		Spliced	Unspliced	
pJTM14	0	82	18	1	44	56	1
	3	84	16	2	48	52	6
	6	85	15	2	50	50	4
	9	90	10	9	54	46	4
	12	84	16	2	60	40	3
pJTM21	0	53	47	7	57	43	4
	3	53	47	3	57	43	5
	6	53	47	5	57	43	5
	9	47	53	3	52	48	3
	12	52	48	0	54	46	1
pJTM28	0	53	47	3	54	46	3
	3	44	56	1	57	43	2
	6	37	63	3	64	36	3
	9	45	55	5	67	33	1
	12	ND[e]	ND	ND	ND	ND	ND
pΔ5-14 3'CAT	0	43	57	2	84	16	2
	3	44	56	3	93	7	2
	6	45	55	1	92	8	2
	9	49	51	10	94	5	3
	12	36	64	2	95	5	2

[a] RNase protection assays for 3' processing and splicing were carried out as described in the legend to Fig. 1 and in Materials and Methods.
[b] Time at which the RNA was harvested after the addition of dactinomycin.
[c] The standard deviation resulting from a duplicate experiment with each pair [viral poly(A) and read-through RNAs; spliced and unspliced RNAs].
[d] RT, RNA which read through the ASV poly(A) signal.
[e] ND, not done.

TABLE 2. Effect of SV40 small-t intron on 3' processing levels[a]

Clone	% RNA processed		SD[b]	% RNA processed		SD
	With small-t intron			Without small-t intron		
	At 3' LTR	As RT[c]		At 3' LTR	As RT	
pJTM14	84	16	5	87	13	4
pJTM21	51	49	12	54	46	NA[d]
pJTM28	50	50	8	50	50	NA

[a] RNase protection assays for 3' processing were carried out as described in the legend to Fig. 1 and in Materials and Methods.
[b] The standard deviation resulting from two or more experiments with each pair [viral poly(A) and read-through RNAs].
[c] RT, RNA which read through the ASV poly(A) signal.
[d] NA, not applicable. These data were based on the results of one experiment.

slightly, but significantly, elevated (25% versus 16%; $P < 0.05$), compared with the levels of wild-type (Fig. 1B, lane 5; Fig. 2). Several mutations in the region of the *src* 3' ss were also examined. One mutant (pMPM13) contained a 4-nt deletion encompassing the *src* 3' ss at nt 7054, preventing splicing at the *src* 3' ss. This construct demonstrated an increase in the amount of unspliced RNA, with little or no change in the amount of *env* message (4). Similar results were obtained by using a mutant deleted between nt 6983 and nt 7127 (data not shown). Another mutant (pJTM46) contained a 22-nt deletion upstream of the *src* 3' ss, which was previously shown to demonstrate an approximately twofold increase in the amount of spliced *src* mRNA with a concomitant decrease in the level of unspliced RNA (4). The amount of viral RNA resulting from read-through of the viral poly(A) site obtained with any of the above three clones was not significantly different ($P > 0.1$) from that of the wild type (Fig. 2).

In order to further test the relationship of ASV RNA splicing to 3'-end formation, we examined two additional constructs which would not be expected to undergo splicing. First, we investigated a mutant which combined the pMPM7 *env* 3' ss mutation and pMPM13 *src* 3' ss mutation (pJTM77). This clone, as expected, demonstrated little or no splicing by using the ASV 5' ss (data not shown) but exhibited levels of read-through RNA comparable to those of the wild-type clone (Fig. 2). Because the limited number of repetitions did not allow us to determine statistical significance, we cannot yet determine whether there is a slight elevation of read-through RNA with pJTM77 similar to that with the *env* 3' ss mutant pMPM7 (Fig. 2). Second, we studied a *src* cDNA clone (pJS2CAT) that does not require splicing in order to express *src* mRNA and which lacks both regions I and II. This clone demonstrated levels of read-through RNA comparable to those of spliceable clones deleted in both regions (Fig. 1C, lane 7; Fig. 2). These results suggested that the extent of read-through RNA transcription is not directly coupled to the act of splicing but to the absence of *cis* elements in region I or II or both.

In all of the above constructs, the sequence downstream of the 3' LTR contained the intron of the SV40 small-t antigen. The presence of this intron in the 3' untranslated region of a gene has been shown, in some cases, to inhibit gene expression at the posttranscriptional level and to cause aberrant splicing (24). In order to determine whether this intron was influencing 3'-end formation, both wild-type and mutant constructs that contained an appropriately sized *src* exon fragment (nt 7127 to 7736) substituted for the above sequence were examined by the RNase protection assay. The amounts of read-through RNA detected with the wild-type (13% versus 16%), region I (54% versus 49%), or region II (50% versus 50%) deletions were comparable to those obtained with constructs containing the small-t antigen intron, suggesting that the presence of this intron does not influence 3'-end formation in this assay (Table 2).

Read-through transcripts are present in both spliced and unspliced RNA pools. To confirm the RNase protection assay results and to examine the proportion of read-through transcripts present in the spliced and unspliced pools of RNA from transfected cells, Northern blot analysis was performed with the probe diagrammed in Fig. 1A (Fig. 4). The expected sizes for the read-through transcripts which were cleaved and polyadenylated at the SV40 poly(A) site downstream is approximately 1.6 kb larger than the correctly processed RNAs. As expected, the wild-type construct, pJTM14, exhibited a low level of unspliced read-through products present in the 10.9-kb band. The same was true for a clone deleted in the 3' *gag* and 5' *pol* genes (pJTM29, 8.9 kb). An elevated level of unspliced read-through transcripts compared with that of the wild type was present in clones which were mutated in region I (pJTM21, 9.6 kb; pJTM50, 10.9 kb) or II (pJTM28, 10.8 kb). It was difficult to detect the amount of spliced read-through products because of the low amount of total spliced RNA in all of these clones. However, it was clear from the data obtained with mutants with which the amount of splicing was significantly increased that both the spliced and unspliced pools of RNA contained read-through transcripts which were processed at the SV40 poly(A) site.

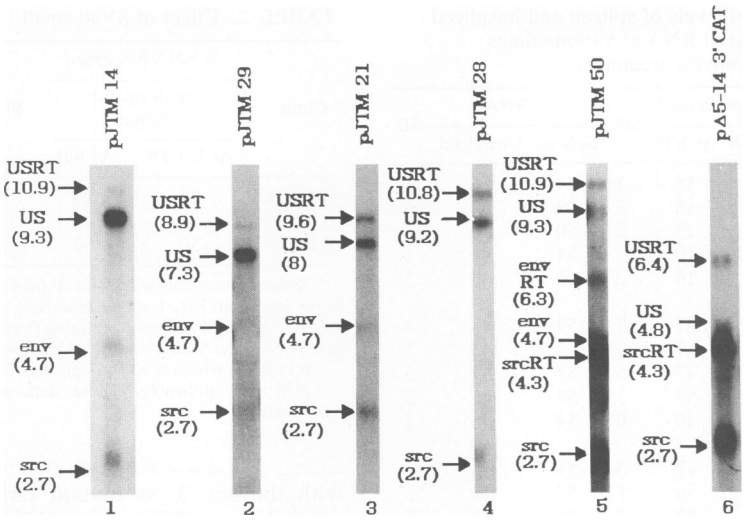

FIG. 4. Northern blot analysis of RNA from CEF transfected with wild-type and mutant constructs. The genomic (US) and subgenomic (*env* and *src*) RNA species are indicated, as well as the corresponding read-through products (RT), if present. The sizes (in kilobases) of the various RNA transcripts are indicated in parentheses.

The inversion mutant pJTM50 demonstrated elevated levels of read-through products resulting from the spliced pools (*env*, 6.3 kb, and *src*, 4.3 kb) as well as from the unspliced pools (10.9 kb). The region I-region II deletion mutant pΔ5-14 3'CAT demonstrated the same phenomenon for the spliced *src* RNA (4.3 kb). In this case, the ratio of *src* read-through products processed at the SV40 poly(A) site to correctly processed *src* RNAs appeared to be somewhat lower than the values detected by the RNase protection assay, the results of which are shown in Fig. 2. One explanation may be that Northern blot analysis is able to clearly detect only those transcripts which are complete, whereas RNase protection can detect nicked species, leading to a value higher than that detected by the Northern blot. In addition, the large amount of 28S rRNA which migrates similarly may interfere with transfer or hybridization of the probe to the 4.3-kb read-through RNA species. Alternatively, there may be transcripts which have been processed at heterologous locations downstream that are not readily detectable by Northern blot analysis.

The effect of upstream sequences on 3'-end processing of ASV RNA can be alleviated by substitution of a heterologous poly(A) signal. In order to determine whether the requirement for regions I and II was specific to the ASV poly(A) site, constructs in which an efficient heterologous poly(A) signal was substituted for the viral poly(A) site were created (Fig. 5A). These constructs contained the *cat* and SV40 downstream sequences. Clone pJTM60 contains the SV40 early poly(A) signal in place of the ASV signal; the remainder of the plasmid is identical to the wild-type clone. Northern blot analysis revealed that less than 1% of viral RNAs resulted from read-through transcription and were processed at the downstream SV40 poly(A) site (compare the 10.9-kb band in Fig. 4, lane 1, to that in Fig. 5B, lane 3). This result suggested that the SV40 early poly(A) signal is more efficient than the ASV poly(A) signal. To determine whether region I or II or both were required for this efficient 3'-end processing, mutant constructs containing the SV40 early poly(A) signal were examined (Fig. 5A, pJTM58 and pJTM62). The amount of read-through transcripts detected with either of these mutants was negligible (Fig. 5B, lanes 4 and 5; compare to either the deletion mutant pΔ5-25 3'CAT or the *src* cDNA clone pJS2CAT, Fig. 5B, lanes 1 and 2), suggesting that neither region I alone nor regions I and II together were required for this efficient 3'-end processing. RNA from cells transfected with constructs identical to the above clones containing the SV40 late poly(A) signal instead of the ASV poly(A) signal was also examined by Northern blot analysis, with similar results (data not shown). To confirm the results obtained by Northern blot analysis, an RNase protection assay was performed with the above RNA samples with the antisense riboprobes spanning the SV40 early or late poly(A) sites. The amount of read-through products was less than 1% of the total amount of viral RNA transcripts. Conversely, genomic clones deleted in region I or II or both containing the ASV 3' LTR poly(A) site, as expected from the previous data, demonstrated an elevated level of RNA transcripts processed at the downstream SV40 early poly(A) site (data not shown). These data suggest that the ability of the upstream regions to facilitate 3'-end formation is specific for the relatively weak ASV poly(A) signal.

DISCUSSION

The results show that the efficiency of 3'-end processing at the ASV poly(A) addition site in the 3' LTR is reduced by the deletion of two distant upstream regions. Region I mapped to the *gag* gene between nt 630 and 1149 and contained both an NRS (2, 54) and an enhancer element (3, 27, 52), either of which may coincide with the sequences responsible for the effects on viral 3'-end processing. The effect on 3'-end formation was absolutely dependent on a positive orientation. Therefore, it is possible that the NRS, whose effect on splicing is also absolutely orientation dependent (2), is responsible for the phenomenon, but further work is required to map more precisely the *cis* element responsible for the effect. Region II was located in the 3' *pol* and 5' *env* sequences between nt 4995 and 5131 and contains the *env* 3' ss at nt 5078 (11, 48). This region also contains part of an element shown by deletion to be important in regulating ASV splicing (29). The importance of the 3' *pol*–5' *env* region in determining the efficiency of 3'-end processing of

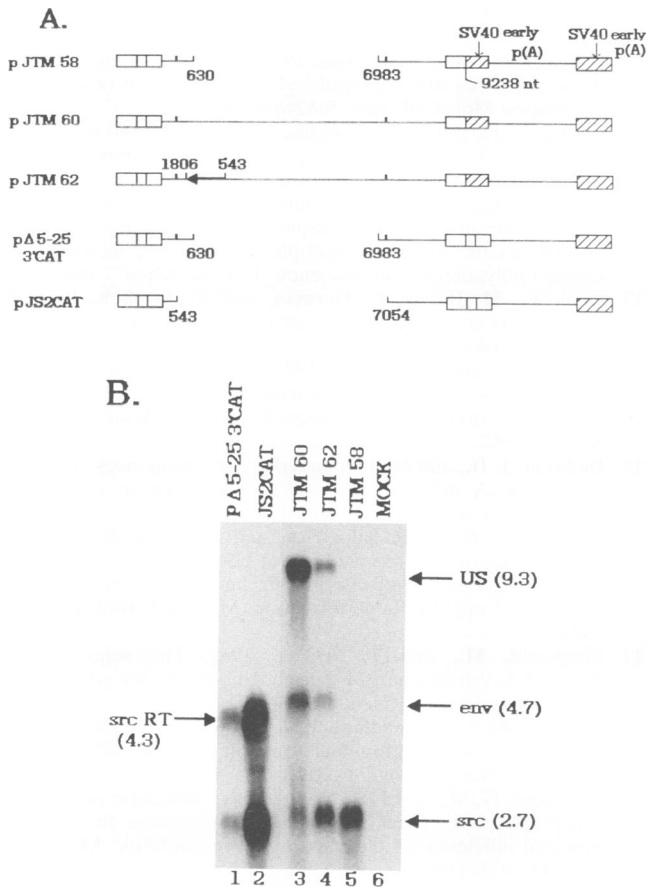

FIG. 5. Effect of substituting of a heterologous poly(A) signal on RSV 3′-end formation. (A) Schematic representation of clones with the inserted SV40 gene fragment containing the early poly(A) signal. The wild type (pJTM60), an inversion of region I (pJTM62), and a deletion of regions I and II (pJTM58) are shown. (B) Northern blot analysis of RNA from CEF transiently transfected with the constructs diagrammed in panel A. An *src* cDNA clone (pJS2CAT) and a region I and region II deleted mutant (pΔ5-25 3′CAT), both containing the RSV poly(A) signal, are also shown for comparison. Identities and sizes of the bands indicated are as described in the legend to Fig. 4.

ASV RNA was previously suggested by the experiments of Wang (59), who showed that the presence of aberrantly large RNA species in CEF cell lines transformed by defective ASV correlated with deletion of this region. This result was shown to be a *cis* effect and could not be complemented by expression of a helper virus genome. The aberrant RNA species contained cellular sequences at their 3′ ends, resulting from read-through transcription followed by cleavage and polyadenylation at cellular processing sites downstream of the integrated proviruses.

Our data indicated that, although both regions I and II contained *cis* elements that influenced the level of viral RNA splicing (2, 28, 29, 54), the increased level of read-through transcripts was not directly coupled to the act of viral RNA splicing. Previous studies have indicated that 3′ cleavage and polyadenylation of other cellular and viral RNA polymerase II transcripts may be facilitated by the presence of *cis* splicing signals. Several studies showed that the presence of introns in a transcriptional unit are associated with significant increases in the level of expression of the gene (12, 13, 23, 37). One study has shown that this increased level of expression was not correlated with the level of transcription but with the level of poly(A)$^+$ RNA in the nucleus (23). This poly(A)$^+$ RNA included both unspliced precursors and spliced RNA species, suggesting that the increase in efficiency of 3′-end processing was correlated with the potential of the RNA to be spliced, i.e., the presence of functional splice sites, rather than with the splicing event itself. Results from a coupled in vitro splicing and polyadenylation system have also supported a role for splice sites in determining the efficiency of 3′-end processing. It was found that the rate of 3′-end processing was stimulated when RNA substrates containing introns were used. This effect required an intact 3′ ss but not a 5′ ss, suggesting that the presence of the 3′ ss processing signals and the ability to "define" the terminal exon rather than splicing itself may determine 3′-end processing efficiency (36). Recent in vivo studies involving the SV40 late leader sequences by Chiou et al. (12) have supported these data, by finding that the decrease in the level of polyadenylation efficiency was more pronounced when mutant upstream 3′ ss were present, rather than when upstream 5′ ss were mutated. The previous studies (12, 36) showed that increased 3′-end processing efficiency was correlated with the presence of a functional 3′ ss that was upstream of the AAUAAA hexanucleotide and flanked the 3′ terminal exon of the pre-mRNA. It is interesting to note that this finding was not the case in our system. Mutation or deletion of the *src* 3′ ss did not affect the efficiency of 3′-end processing at the ASV poly(A) site. Rather, deletion of a fragment containing the more distal *env* 3′ ss exhibited the lower 3′-end processing phenotype. Under these conditions, the presence of an intact *src* 3′ ss was not sufficient to maintain wild-type 3′-end formation efficiency. These results suggest that 3′-end formation in retroviruses may require a selective interaction between specific splicing signals and the viral poly(A) site. These different rules for 3′-end processing may apply to retroviruses, which must maintain a significant pool of unspliced RNA, in contrast to those that apply to cellular pre-mRNAs, which are almost completely spliced.

The striking effect of upstream sequences on the efficiency of ASV RNA 3′ processing may result from the relative weakness of the 3′ LTR poly(A) signal. Consistent with this hypothesis, we found that when the viral 3′ LTR poly(A) signal was replaced with the efficient SV40 early or late poly(A) signal, the requirement for the upstream sequences was alleviated and read-through transcription was essentially eliminated. Alternatively, this result may indicate that 3′-end processing in ASV requires more-specific interactions between the 3′ LTR poly(A) site and the upstream sequences to maintain cleavage and polyadenylation at wild-type levels than are required for the SV40 signals.

The efficiency of 3′-end processing has been correlated with the binding of a cleavage factor to the GU- or U-rich element downstream of the poly(A) cleavage site. The sequence of this element is highly variable in different poly(A) sites, and these differences in sequence apparently determine the level of factor binding (19, 61). One possible explanation for the effect of the upstream ASV sequences on the efficiency of 3′-end processing could be that the upstream sequences bind additional factors that interact with the cleavage factor to stabilize its binding to the viral poly(A) addition site. Since region II contains part of a splicing regulatory element and the *env* 3′ ss, these additional factors may be splicing factors. The mechanism by which the NRS element in region I acts to inhibit splicing is also not yet

known. One possible model is that the NRS inhibits splicing by acting as a "decoy" splice site that competes with the authentic splice site for splicing factors (51). Thus, the NRS element in region I may also bind splicing factors that interact with factors bound at the poly(A) addition site. Alternatively, region I or II or both may contain secondary structure elements that are recognized by the 3′ processing complex in order to achieve efficient cleavage and polyadenylation at the viral poly(A) site.

There have been several previous reports indicating that 3′-end processing of other retroviruses and pararetroviruses is dependent on upstream sequences within 500 nt of the poly(A) signal (9, 16, 42, 43, 46, 57); however, these upstream sequences do not appear to contain splicing signals. It is possible that ASV may also contain such elements; we would not have detected their effect in our studies since we have analyzed 3′-end processing in the presence of the region which corresponds in location to these previously defined elements. In a series of experiments analyzing the genome of the *Drosophila melanogaster* retrotransposon *copia*, it has been found that deletion of a 518-nt region beginning 312 nt upstream from the 3′-end processing site inhibits cleavage and polyadenylation at the *copia* 3′ LTR and results in an increase in the amount of read-through transcripts (30). The deleted region contains a 3′ ss, which is used to synthesize a subgenomic *copia* mRNA. The 3′-end processing of both the unspliced and the spliced 2-kb *copia* RNAs was affected by deletion of this region, suggesting the possibility that a region containing *cis*-acting splicing signals may, in this case, facilitate *copia* 3′-end processing by a mechanism similar to that proposed above for ASV RNA.

ACKNOWLEDGMENTS

This work was supported by Public Health Service grant CA28051 from the National Cancer Institute.

We thank S. Perlman, M. F. Stinski, and the members of our laboratory for critical review of the manuscript and M. Reeve for typing.

REFERENCES

1. **Adami, G., and J. R. Nevins.** 1988. Splice site selection dominates over poly(A) site choice in RNA production from complex adenovirus transcription units. EMBO J. **7:**2107–2116.
2. **Arrigo, S., and K. Beemon.** 1988. Regulation of Rous sarcoma virus splicing and stability. Mol. Cell. Biol. **8:**4858–4867.
3. **Arrigo, S., M. Yun, and K. Beemon.** 1987. *cis*-acting regulatory elements within the *gag* gene of avian retroviruses. Mol. Cell. Biol. **7:**388–397.
4. **Berberich, S. L., and C. M. Stoltzfus.** 1991. Mutations in the regions of the Rous sarcoma virus 3′ splice sites: implications for regulation of alternative splicing. J. Virol. **65:**2640–2646.
5. **Bhat, B. M., and W. S. Wold.** 1985. AATAAA as well as downstream sequences are required for RNA 3′-end formation in E3 complex transcription unit of adenovirus. Mol. Cell. Biol. **5:**3183–3193.
6. **Bingham, P. M., and Z. Zachar.** 1989. Retrotransposons and the FB transposon from *Drosophila melanogaster*, p. 485–502. *In* D. E. Berg and M. M. Howe (ed.), Mobile DNA. American Society for Microbiology, Washington, D.C.
7. **Bohnlein, S., J. Hauber, and B. R. Cullen.** 1989. Identification of a U5-specific sequence required for efficient polyadenylation within the human immunodeficiency virus long terminal repeat. J. Virol. **63:**421–424.
8. **Brady, H. A., and W. S. M. Wold.** 1988. Competition between splicing and polyadenylation reactions determines which adenovirus region E3 mRNAs are synthesized. Mol. Cell. Biol. **8:**3291–3297.
9. **Brown, P. H., L. S. Tiley, and B. R. Cullen.** 1991. Efficient polyadenylation within the human immunodeficiency virus type 1 long terminal repeat requires flanking U3-specific sequences. J. Virol. **65:**3340–3343.
10. **Carswell, S., and J. C. Alwine.** 1989. Efficiency of utilization of the simian virus 40 late polyadenylation site: effects of upstream sequences. Mol. Cell. Biol. **9:**4248–4258.
11. **Chang, L.-J., and C. M. Stoltzfus.** 1985. Cloning and nucleotide sequences of cDNAs spanning the splice junctions of Rous sarcoma virus mRNAs. J. Virol. **53:**969–972.
12. **Chiou, H. C., C. Dabrowski, and J. C. Alwine.** 1991. Simian virus 40 late mRNA leader sequences involved in augmenting mRNA accumulation via multiple mechanisms, including increased polyadenylation efficiency. J. Virol. **65:**6677–6685.
13. **Choi, T., M. Huang, C. Gorman, and R. Jaenisch.** 1991. A generic intron increases gene expression in transgenic mice. Mol. Cell. Biol. **11:**3070–3074.
14. **Conway, L., and M. Wickens.** 1985. A sequence downstream of AAUAAA is required for formation of simian virus 40 late mRNA 3′ termini in frog oocytes. Proc. Natl. Acad. Sci. USA **82:**3949–3952.
15. **DeZazzo, J. D., and M. J. Imperiale.** 1989. Sequences upstream of AAUAAA influence poly(A) site selection in a complex transcription unit. Mol. Cell. Biol. **9:**4951–4961.
16. **DeZazzo, J. D., J. E. Kilpatrick, and M. J. Imperiale.** 1991. Involvement of long terminal repeat U3 sequences overlapping the transcriptional control region in human immunodeficiency virus type 1 mRNA 3′-end formation. Mol. Cell. Biol. **11:**1624–1630.
17. **Fitzgerald, M., and T. Schenk.** 1981. The sequence 5′-AAUAAA-3′ forms part of the recognition site for polyadenylation of late SV40 mRNAs. Cell **24:**251–260.
18. **Gil, A., and N. J. Proudfoot.** 1984. A sequence downstream of AAUAAA is required for efficient rabbit β-globin mRNA 3′-end formation. Nature (London) **312:**473–474.
19. **Gilmartin, G. M., and J. R. Nevins.** 1991. Molecular analyses of two poly(A) site-processing factors that determine the recognition and efficiency of cleavage of the pre-mRNA. Mol. Cell. Biol. **11:**2432–2438.
20. **Helfman, D. M., S. Cheley, E. Kuismanen, L. A. Finn, and Y. Yamawaki-Kataoka.** 1986. Nonmuscle and muscle tropomyosin isoforms are expressed from a single gene by alternative RNA splicing and polyadenylation. Mol. Cell. Biol. **6:**3582–3595.
21. **Herman, S. A., and J. M. Coffin.** 1986. Differential transcription from the long terminal repeats of integrated avian leukosis virus DNA. J. Virol. **60:**497–505.
22. **Herman, S. A., and J. M. Coffin.** 1987. Efficient packaging of readthrough RNA in ALV. Implications for oncogene transduction. Science **236:**845–848.
23. **Huang, M. T. F., and C. M. Gorman.** 1990. Intervening sequences increase efficiency of RNA 3′ processing and accumulation of cytoplasmic RNA. Nucleic Acids Res. **18:**937–947.
24. **Huang, M. T. F., and C. M. Gorman.** 1990. The simian virus 40 small-t intron, present in many common expression vectors, leads to aberrant splicing. Mol. Cell. Biol. **10:**1805–1810.
25. **Iwasaki, K., and H. M. Temin.** 1990. The efficiency of RNA 3′-end formation is determined by the distance between the cap site and the poly(A) site in spleen necrosis virus. Genes Dev. **4:**2299–2307.
26. **Kanter, M. R., R. E. Smith, and W. S. Hayward.** 1988. Rapid induction of B-cell lymphomas: insertional activation of *c-myb* by avian leukosis virus. J. Virol. **62:**1423–1432.
27. **Karnitz, L., S. Faber, and R. Chalkley.** 1987. Specific nuclear proteins interact with Rous sarcoma virus internal enhancer and share a common element with the enhancer located in the long terminal repeat of the virus. Nucleic Acids Res. **15:**9841–9859.
28. **Katz, R. A., M. Kotler, and A. M. Skalka.** 1988. *cis*-acting intron mutations that affect the efficiency of avian retroviral RNA splicing: implications for mechanisms of control. J. Virol. **62:**2686–2695.
29. **Katz, R. A., and A. M. Skalka.** 1990. Control of retroviral RNA splicing through maintenance of suboptimal processing signals. Mol. Cell. Biol. **10:**696–704.
30. **Kurkulos, M., J. M. Weinberg, M. E. Pepling, and S. M. Mount.** 1991. Polyadenylation in *copia* requires unusually distant up-

stream sequences. Proc. Natl. Acad. Sci. USA **88:**3038–3042.
31. **Leff, S. E., R. M. Evans, and M. G. Rosenfeld.** 1987. Splice site commitment dictates neuron-specific alternative RNA processing in calcitonin/CGRP gene expression. Cell **48:**517–524.
32. **McDevitt, M. A., R. P. Hart, W. W. Wong, and J. R. Nevins.** 1986. Sequences capable of restoring poly(A) site function define two distinct downstream elements. EMBO J. **5:**2907–2913.
33. **McDevitt, M. A., M. J. Imperiale, H. Ali, and J. R. Nevins.** 1984. Requirement of a downstream sequence for generation of a poly(A) addition site. Cell **37:**993–999.
34. **Melton, D. A., P. A. Kreig, M. R. Rebagliati, T. Maniatis, K. Zinn, and M. R. Green.** 1984. Efficient *in vitro* synthesis of biologically active RNA and RNA hybridization probes from plasmids containing the bacteriophage SP6 promoter. Nucleic Acids Res. **12:**7035–7056.
35. **Montell, C., E. F. Fisher, M. H. Caruthers, and A. J. Berk.** 1983. Inhibition of RNA cleavage but not polyadenylation by a point mutation in mRNA 3' consensus sequence AAUAAA. Nature (London) **305:**600–629.
36. **Niwa, M., S. D. Rose, and S. M. Berget.** 1990. *In vitro* polyadenylation is stimulated by the presence of an upstream intron. Genes Dev. **4:**1552–1559.
37. **Palmiter, R. D., E. P. Sandgren, M. R. Avarbock, D. D. Allen, and R. Brinster.** 1991. Heterologous introns can enhance expression of transgenes in mice. Proc. Natl. Acad. Sci. USA **88:**478–482.
38. **Peterson, M. L., E. R. Gimmi, and R. P. Perry.** 1991. The developmentally regulated shift from membrane to secreted μ mRNA production is accompanied by an increase in cleavage-polyadenylation efficiency but no measurable change in splicing efficiency. Mol. Cell. Biol. **11:**2324–2327.
39. **Proudfoot, N. J.** 1991. Poly(A) signals. Cell **64:**671–674.
40. **Proudfoot, N. J., and G. G. Brownlee.** 1976. 3' noncoding region sequences in eukaryotic messenger RNA. Nature (London) **263:**211–214.
41. **Raines, M. A., N. J. Maihle, C. Moscovici, L. Crittenden, and H.-J. Kung.** 1988. Mechanism of c-*erbB* transduction: newly released transducing viruses retain poly(A) tracts of *erbB* transcripts and encode C-terminally intact *erbB* proteins. J. Virol. **62:**2437–2443.
42. **Russnak, R. H.** 1991. Regulation of polyadenylation in hepatitis B viruses: stimulation by the upstream activating signal PS1 is orientation-dependent, distance-independent, and additive. Nucleic Acids Res. **19:**6449–6456.
43. **Russnak, R., and D. Ganem.** 1990. Sequences 5' to the polyadenylation signal mediate differential poly(A) site use in hepatitis B viruses. Genes Dev. **4:**764–776.
44. **Sadofsky, M., S. Connelly, J. L. Manley, and J. Alwine.** 1986. Identification of a sequence element on the 3' side of AAUAAA which is necessary for simian virus 40 late mRNA 3'-end processing. Mol. Cell. Biol. **5:**2713–2719.
45. **Sambrook, J., E. F. Fritsch, and T. Maniatis.** 1989. Molecular cloning: a laboratory manual, 2nd ed. Cold Spring Harbor Laboratory, Cold Spring Harbor, N.Y.
46. **Sanfacon, H., P. Brodmann, and T. Hohn.** 1991. A dissection of the cauliflower mosaic virus polyadenylation signal. Genes Dev. **5:**141–149.
47. **Sanfacon, H., and T. Hohn.** 1990. Proximity to the promoter inhibits recognition of cauliflower mosaic virus polyadenylation signal. Nature (London) **346:**81–84.
48. **Schwartz, D. E., R. Tizard, and W. Gilbert.** 1983. Nucleotide sequence of Rous sarcoma virus. Cell **32:**853–869.
49. **Simonsen, C. C., and A. D. Levinson.** 1983. Analysis of processing and polyadenylation signals of the hepatitis B virus surface antigen gene by using simian virus 40-hepatitis B virus chimeric plasmids. Mol. Cell. Biol. **3:**2250–2258.
50. **Sompayrac, L. M., and K. Danna.** 1981. Efficient infection of monkey cells with DNA and SV40. Proc. Natl. Acad. Sci. USA **78:**7575–7578.
51. **Stoltzfus, C. M.** 1988. Synthesis and processing of avian sarcoma retrovirus RNA. Adv. Virus Res. **35:**1–38.
52. **Stoltzfus, C. M., L.-J. Chang, T. P. Cripe, and L. P. Turek.** 1987. Efficient transformation by Prague A Rous sarcoma virus plasmid DNA requires the presence of *cis*-acting regions within the *gag* gene. J. Virol. **61:**3401–3409.
53. **Stoltzfus, C. M., K. Dimock, S. Horikami, and T. Ficht.** 1983. Stabilities of avian sarcoma virus RNAs: comparison of subgenomic and genomic species with cellular mRNAs. J. Gen. Virol. **64:**2191–2202.
54. **Stoltzfus, C. M., and S. J. Fogarty.** 1989. Multiple regions in the Rous sarcoma virus *src* gene intron act in *cis* to affect the accumulation of unspliced RNA. J. Virol. **63:**1669–1676.
55. **Strohman, R., P. Moss, J. Micou-Eastwood, D. Spector, A. Przybyla, and B. Peterson.** 1977. Messenger RNA for myosin polypeptides: isolation from single myogenic cell cultures. Cell **10:**265–273.
56. **Swain, A., and J. M. Coffin.** 1992. Mechanism of transduction by retroviruses. Science **255:**841–845.
57. **Valsamakis, A., S. Zeichner, S. Carswell, and J. C. Alwine.** 1991. The human immunodeficiency virus type 1 polyadenylation signal: a 3' long terminal repeat element upstream of the AAUAAA necessary for efficient polyadenylation. Proc. Natl. Acad. Sci. USA **88:**2108–2112.
58. **Wang, J., and T. Pederson.** 1990. A 62,000 molecular weight spliceosome protein crosslinks to the intron polypyrimidine tract. Nucleic Acids Res. **18:**5995–6001.
59. **Wang, L.-H.** 1985. Deletion in the 3' *pol* sequence correlates with aberration of RNA expression in certain replication-defective avian sarcoma viruses. J. Virol. **54:**446–459.
60. **Weichs an der Glon, C., J. Monks, and N. J. Proudfoot.** 1991. Occlusion of the HIV poly(A) site. Genes Dev. **5:**244–253.
61. **Weiss, E. A., G. M. Gilmartin, and J. R. Nevins.** 1991. Poly(A) site efficiency reflects the stability of complex formation involving the downstream element. EMBO J. **10:**215–219.
62. **Wickens, M., and P. Stephenson.** 1984. Role of the conserved AAUAAA sequence: four AAUAAA point mutants prevent messenger RNA 3'-end formation. Science **226:**1045–1051.
63. **Wickens, M.** 1990. How the messenger got its tail: addition of poly(A) in the nucleus. Trends Biochem. Sci. **15:**277–281.
64. **Zhang, F., R. M. Denome, and C. N. Cole.** 1986. Fine structure analysis of the processing and polyadenylation region of the herpes simplex virus type 1 thymidine kinase gene by using linker scanning, internal deletion, and insertion mutations. Mol. Cell. Biol. **6:**4611–4623.